COBEM 2023 27TH INTERNATIONAL CONGRESS OF MECHANICAL ENGINEERING

ABCM Brazilian Society of Mechanical Sciences and Engineering
27th ABCM International Congress of Mechanical Engineering
December 04-08, 2023, Florianópolis-SC, Brazil

COB-2023-2419
EXPERIMENTAL STUDY OF A HORIZONTAL LIQUID FILM HEAT EXCHANGER CONFIGURATION

Beethoven Narváez-Romo
betonarmo@usp.br
José R. Simões-Moreira
jrsimoes@usp.br
SISEA - Renewable and Alternative Energy Systems Laboratory, Escola Politécnica at University of São Paulo, Brazil

Abstract. *Flooded and falling film evaporators are commonly used in various engineering applications. In terms of heat transfer performance, falling liquid film has higher values than flooded evaporators. However, the wettability problems are still present in liquid falling film applications. Therefore, this study proposes a new heat exchanger configuration that uses a horizontal liquid film to improve wettability issues. The heat exchanger is composed of several vertically-oriented plates, each of which contains a spiral cooling tube. The secondary fluid flows inside the tube, while the water solution flows over spiral tube to form a horizontal liquid film. The experimental heat rate was computed by using water as working fluid. An overall balance of mass and energy equations was carried out. A set of experimental tests were carried out on the horizontal liquid film in which the inlet water temperature, and its mass flow rate were changed. The heat exchanger was characterized as a function of the mass flow rate and the inlet water temperature. Experimental results showed that heat rejection decreases as the position in the heat exchanger increases. The first group of plates transferred more than 40% of the total heat rate in the exchanger. Although the heat transfer rate increased as the mass flow rate increased, the non-dimensional heat transfer rate slightly changes.*

Keywords: *Wettability, Heat Exchanger, Flooded, Falling film, Heat Transfer*

1. INTRODUCTION

According to Science Direct's database, from 2014-2023, 73,936 documents were published with "falling film" as a keyword, with 26.6%, 11.8% and 1.7% of these studies developed in China, USA, and Brazil, respectively. 39.7% of these studies were related to the engineering field, chemical engineering, and energy, with a particular focus on heat and mass transfer, indicating its significance as a topic in the last decade. Falling film technology has been widely used in various engineering applications, such as absorption refrigeration cycles (Narváez-Romo, 2020, Narváez-Romo et al., 2022), water vaporization processes (Narváez-Romo and Simões-Moreira, 2017), just to mention a few, due to its potential for heat recovery from thermal sources and solar energy (Varón et al., 2023). However, wettability issues continue to be present in liquid falling film applications, which is the main challenge for engineering applications (Ribatski and Jacobi, 2005). Wettability problems may become more severe at extremely low Reynolds numbers, leading to a significant generation of dry-out zones in terms of construction and operation.

Wettability problems in falling film technology have been well studied in the open literature (Fernandes et al., 2017, Ong et al., 2019). One approach to address these issues is to modify the surface properties of the heat exchanger, such as through surface coatings or texturing. For example, a recent study investigated the effects of surface texturing on wettability in a falling film heat exchanger, demonstrating improved liquid spreading and heat transfer performance (Zhang et al., 2021). Another study focused on the use of hydrophilic coatings to improve wettability, reporting enhanced film flow stability and heat transfer coefficients (Xu et al., 2020). These studies highlight the importance of addressing wettability issues in falling film technology, and suggest promising approaches for achieving improved performance.

In this study, a new heat exchanger design is proposed to address wettability issues, utilizing a low-cost spiral configuration that is both compact and suitable for vaporization processes. In contrast to conventional falling film technology, the proposed design does not induce alterations in the boiling temperature resulting from hydrostatic pressure exerted by the liquid column. To evaluate the design, a new horizontal liquid film heat exchanger configuration based on the falling film technology and its wettability problems is experimentally investigated.

2. EXPERIMENTAL TEST RIG

The new proposal for a horizontal liquid film heat exchanger consists of six plates arranged vertically. Each plate contains a spiral cooling tube, as shown in Fig. (1a), through which the water coolant flows inside tube, while the other working fluid (also water) flows over the spiral tube. The plates are placed inside a cylinder, and 1/4 NPT connections are installed over the wall equipment, as shown in Fig. (1b), to link the water coolant between the external and internal

sides. An ABS plate barrier guarantees a one-millimeter horizontal liquid film of the working fluid, and Fig. (1c) shows the horizontal film heat exchanger going over the spiral at the radial direction. It is worthwhile to mention that the proposed design overcomes the wettability issues that are typically found in heat exchangers. Additionally, the proposed design increases the residence time of the working fluid in contact with the heat exchanger, which may reduce the heat transfer coefficient due to lower velocities and a thicker liquid film compared to the conventional falling film technology.

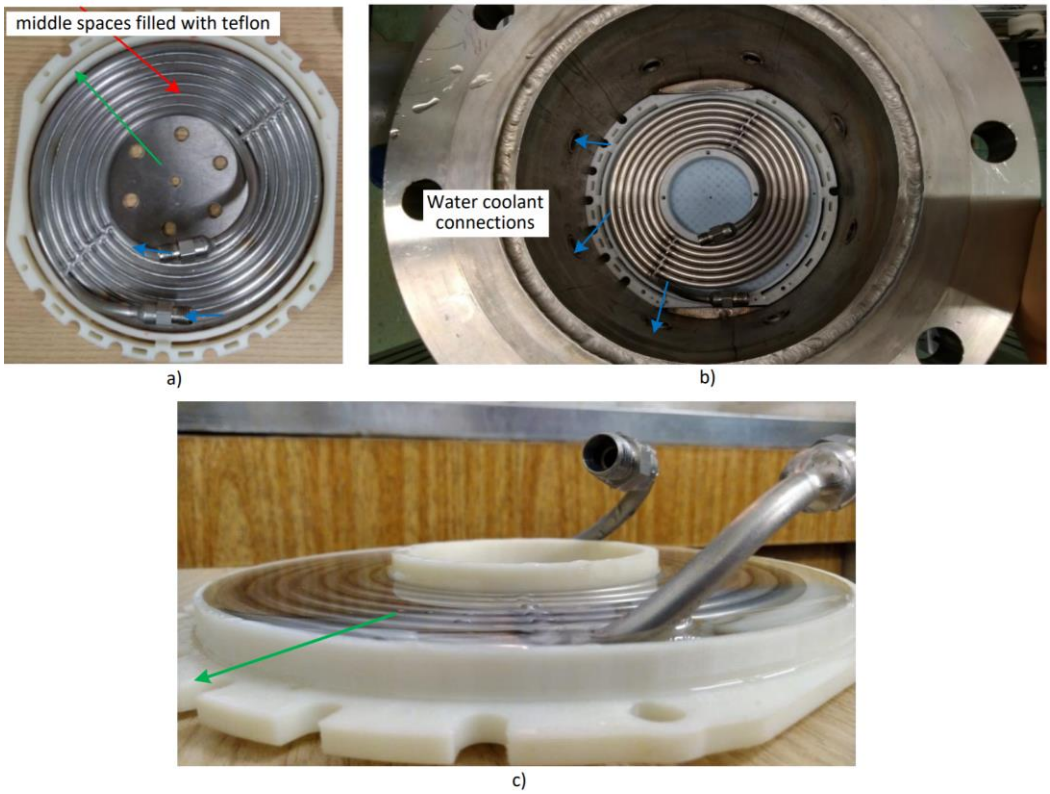

Figure 1 a) Spiral plate, b) spiral plate inside cylinder and c) horizontal liquid film over the spiral plate exchanger.

As shown in Fig. (2), this particular heat exchanger configuration is not commercially available, as it was designed and built on a low budget. A 1/4 stainless steel tube was mounted onto a cylinder fixed to a lathe machine, allowing it to be curved into a spiral shape. Two lateral supports were installed to ensure that the tube was aligned in the Z orthogonal direction. To prevent uncontrolled deformation during the initial turning, a cylindrical wedge was placed over the cylinder, fixing all the tubing coils into place.

Figure 2 Spiral heat exchanger manufacture by shape-lathe process.

Based on the entire heat exchanger project, Fig. (3) displays the manufacturing process of the heat exchanger, which is built using an 8” - 40 Sch 304 stainless steel tube, with two 150 class flanges, 600 length, 16 1/4 NPT connections, and two inspection windows (0.380 m x 0.01 m). The connections are employed in the water coolant circuit, which drives the heat duty of the heat exchanger from each plate (6 plates) to the environment. The six spiral plates are arranged in a vertical position to form a plate column.

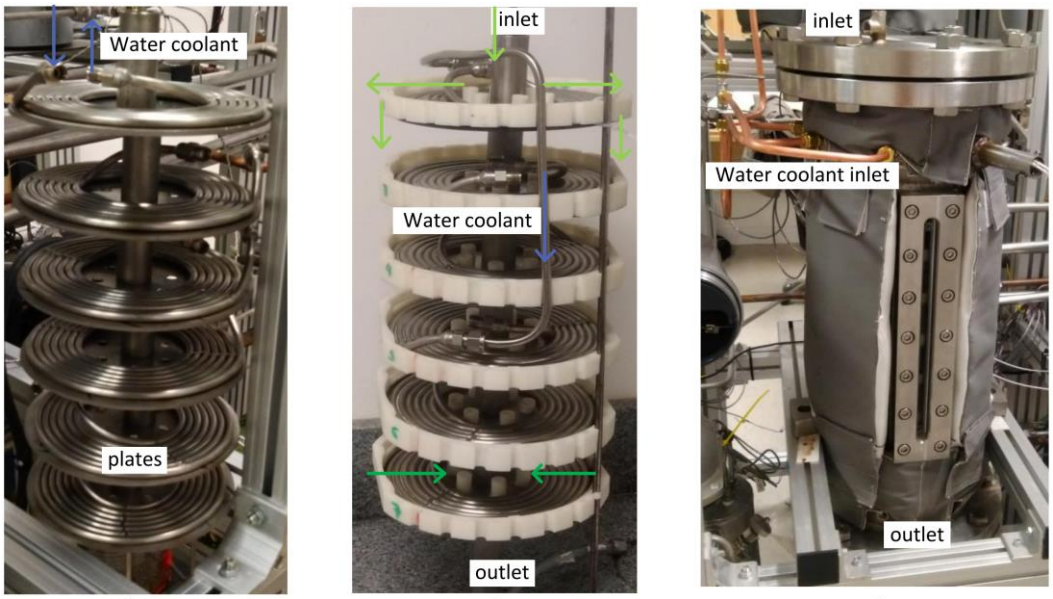

Figure 3 Horizontal liquid film heat exchanger and a) its six plates, b) water cooling connections, and c) final configuration.

Fig. (4) is displayed to provide a better understanding of the external working fluid and water coolant circuits. The diagrams illustrate the external water circuit (M-001), which flows over each heat exchanger plate, and the water coolant circuit that flows inside tubes (M-102). M-001 is distributed over the first plate N1, forming a zig-zag pattern in the subsequent plates (flowing from the outside to the inside in the second plate) until the flow reaches the sixth plate (N6). The temperature measurements of the external water circuit are denoted by T_i and T_o, while T_c stands for temperature of the water coolant circuit at the inlet.

T-type thermocouples with an accuracy of ±0.5°C were used for temperature measurements. External mass flow rate was measured using an Optimass 3000 Coriolis mass flow meter with and uncertainty of ±0.002 kg/s. The volume flow rate of the secondary fluid was measured with a hydrometer, with an uncertainty of ±2.0%. A Lynx ADS-1800 data acquisition system was employed, which has eight universal channels. Uncertainties were determined using Taylor and Kuyatt's method (Klein, 2015) and were calculated using *Engineering Equation Solver* (EES).

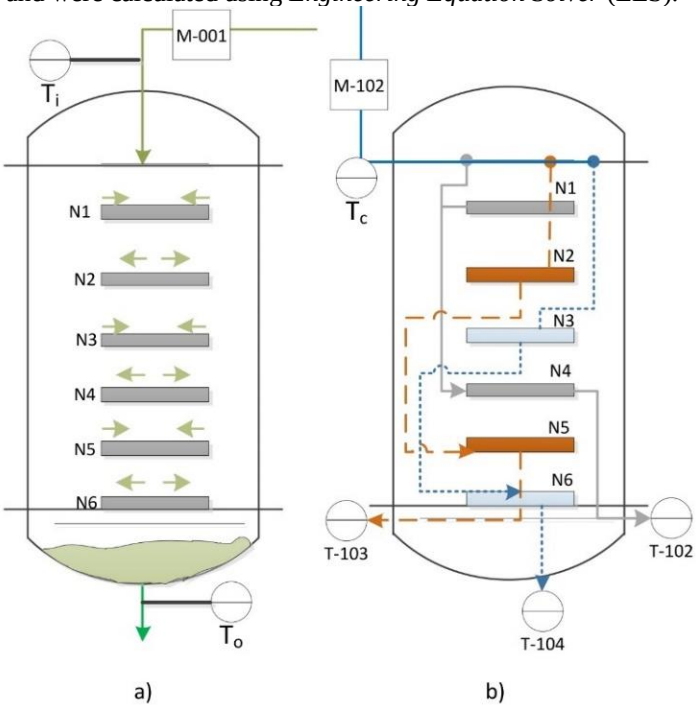

Figure 4 Schematic representation of a horizontal liquid film heat exchanger: a) external water flows over the spiral tube, forming a horizontal liquid film as Fig. (1c), and b) secondary fluid flows inside the tubes for heat transfer.

3. DATA REDUCTION OF HEAT TRANSFER

3.1 Water coolant circuit – internal flow

The total heat rate $\dot{Q}_{\mathrm{HX}}$ absorbed by the water coolant is given by Eq. (1), in which $\dot{Q}_{102}$ is the absorbed heat duty by the $N1$ and $N4$ plates, $\dot{Q}_{103}$ is the absorbed heat duty by the $N2$ and $N5$ plates and $\dot{Q}_{104}$ is the absorbed heat rate by the last group of spiral plates $N3$ and $N6$, or, it is expressed as a function of the total mass flow rate and its average outlet temperature $T_{avg,o}$ as defined in Eq. (2).

$$\dot{Q}_{\mathrm{HX}} = \dot{m}_{102} c_{102}[(T_{102} - T_{101}) + (T_{103} - T_{101}) + (T_{104} - T_{101})] \tag{1}$$

$$\dot{Q}_{\mathrm{HX}} = \dot{m}_{102} c_{102}\left(T_{avg,o} - T_{101}\right) \tag{2}$$

The heat transfer coefficient of the water coolant side is computed by using the Dittus-Boelter's correlation (Dittus, 1930) – Eq. (3), in which it achieves the turbulent regime, which Reynolds number Re_{102} is given by Eq. (4). Prandtl number is defined as a function of the average properties.

$$\mathrm{Nu}_{102} = \frac{\alpha_{102} D_{\mathrm{i}}}{k_{102}} = 0.023 \mathrm{Re}_{102}^{0.8} \mathrm{Pr}_{102}^{0.4} \tag{3}$$

$$\mathrm{Re}_{102} = \frac{4\dot{m}_{102}}{\pi D_{\mathrm{i}} \mu_{102}} \tag{4}$$

The Gnielinski correlation (Gnielinski, 1976) was used for turbulent flow with a 6% accuracy for $\mathrm{Pr} < 200$ (Lienhard, 2011), and it is given by Eq. (5), f stands for the friction factor $f = (1.82 \log_{10}(\mathrm{Re_c} - 1000))^{-2}$. Although the Dittus-Boelter correlation for heat transfer showed less than 5% difference compared to the Gnielinski correlation, this difference is lower than the absolute error of the heat transfer coefficient. Thus, both correlations can be used interchangeably without significantly affecting the computation of the heat transfer coefficient.

$$\mathrm{Nu}_{102} = \left(\frac{f}{8}\right) \frac{\mathrm{Pr}_{102}(\mathrm{Re}_{102} - 1000)}{1 + 12.7\left(\frac{f}{8}\right)(\mathrm{Pr}_{102}^{2/3} - 1)} \tag{5}$$

3.2 Water working fluid – external flow

Based on Fig. (4), mass and energy balances for the control volume are carried out, in which Eq. (6) refers to mass balance and Eq. (7) stands for the energy balance in the external water circuit under steady-state regime. $\dot{m}$ is the mass flow rate, T is the temperature, $c_p$stands for the specific heat capacity at constant pressure, "i" and "o" is the inlet and outlet, respectively.

$$\dot{m}_{001,\mathrm{i}} = \dot{m}_{001,\mathrm{o}} \tag{6}$$

$$\dot{Q}_{\mathrm{HX}} = \dot{m}_{001} c_{p_{001}} (T_o - T_{\mathrm{i}}) \tag{7}$$

Also, $\dot{Q}_{\mathrm{HX}}$ is defined as a function of the global heat transfer coefficient U_{HX}, heat transfer area A_{HX} and the log mean temperature difference $\Delta \mathrm{T}_{\mathrm{LM}}$, in which it is possible to estimate U_{HX} as it is given in Eq. (8). The estimation of a global $\Delta \mathrm{T}_{\mathrm{LM}}$ for the total heat exchanger is given by Eq. (9).

$$U = \frac{\dot{Q}_{\mathrm{tot}}}{A \Delta T_{\mathrm{LM}}} \tag{8}$$

$$\Delta T_{\mathrm{LM}} = \frac{(T_{\mathrm{i}} - T_{\mathrm{c}}) - (T_{\mathrm{o}} - T_{avg,o})}{\ln\left(\frac{T_{\mathrm{i}} - T_{\mathrm{c}}}{T_{\mathrm{o}} - T_{avg,o}}\right)} \tag{9}$$

So, the heat transfer coefficient (α_f) calculation of the horizontal liquid film heat exchanger is carried out by using Eq. (10). D is the tube diameter, U is the global heat transfer coefficient, k refers to the thermal conductivity, α_{c} stands for the heat transfer coefficient in the internal flow.

$$\frac{1}{\alpha_{\mathrm{f}}} = \frac{1}{U} - \left(D_{\mathrm{o}} \frac{\ln\left(\frac{D_{\mathrm{o}}}{D_{\mathrm{i}}}\right)}{2k} + \frac{D_{\mathrm{o}}}{D_{\mathrm{i}}} \frac{1}{\alpha_{\mathrm{c}}} \right) \tag{10}$$

4. RESULTS

Experimental tests were carried out in a co-current configuration, where the coolant working fluid and external water mass flow rate (being cooled) flow down the heat exchanger plates. As shown in Fig. (5), the heat duty increased slightly as the external mass flow rate and inlet temperature increased for both experimental test runs. Although changes in mass flow rate might affect the horizontal liquid film thickness on the plate heat exchanger, it can ensure that all heat exchanger plates are always 1-mm flooded, which explains the increase in heat transfer performance. Moreover, drops that fall from the previous spiral plate can intensify the heat transfer coefficient due to changes in the pattern of the horizontal liquid film. Fluid agitation can mix the streamlines on the plate, which has effects similar to the water feeding of the upper tube in falling film technology. It is well known that the upper tube presents a higher local heat transfer coefficient than the other regions (Chyu and Bergles, 1987; Hu and Jacobi, 1996; Narváez-Romo and Simões-Moreira, 2017), which is known as the impingement jet zone.

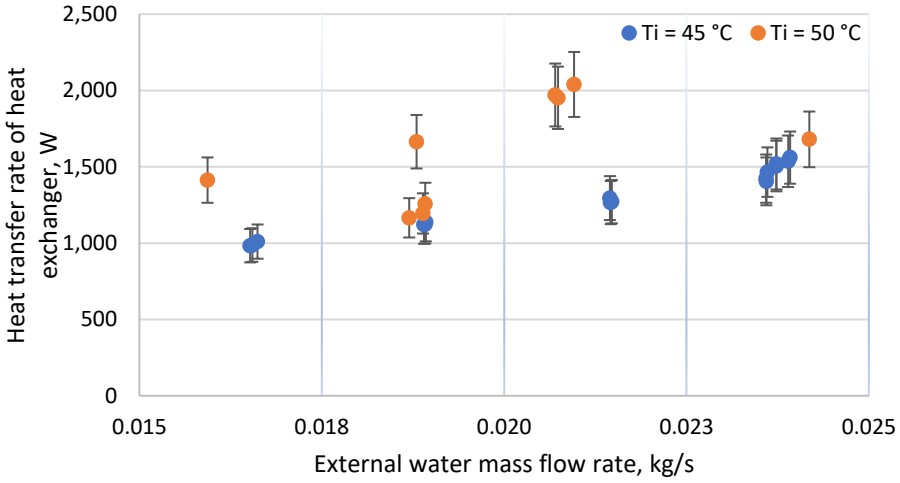

Figure 5 Heat transfer rate as a function of the external water mass flow rate for two inlet temperatures.

Fig. (6) displays the non-dimensional heat rate of each group of heat exchanger plates as a function of the external mass flow rate. Non-dimensional heat rate is defined as the proportion between the heat rate of each group of spiral plates and the total heat rate of heat exchanger ($\dot{Q}_{\mathrm{Ni,Nj}}/\dot{Q}_{\mathrm{tot}}$). For instance, for the first group of heat exchanger plates ($\dot{Q}_{\mathrm{N1N4}}/\dot{Q}_{\mathrm{tot}}$), these plates absorb above 40% of the total heat rate, then, the following group absorbs more than 30% of the total heat rate, and the last group absorbs the other part. It confirms that the heat transfer rates in the beginning of the heat transfer process are intensive due to the high temperature gradient between the water secondary fluid (coolant) and the external water mass flow rate. Moreover, a trade-off between the first group (N1 & N4) and the last group (N3 & N6) of spiral plate occurs when external mass flow rate increases.

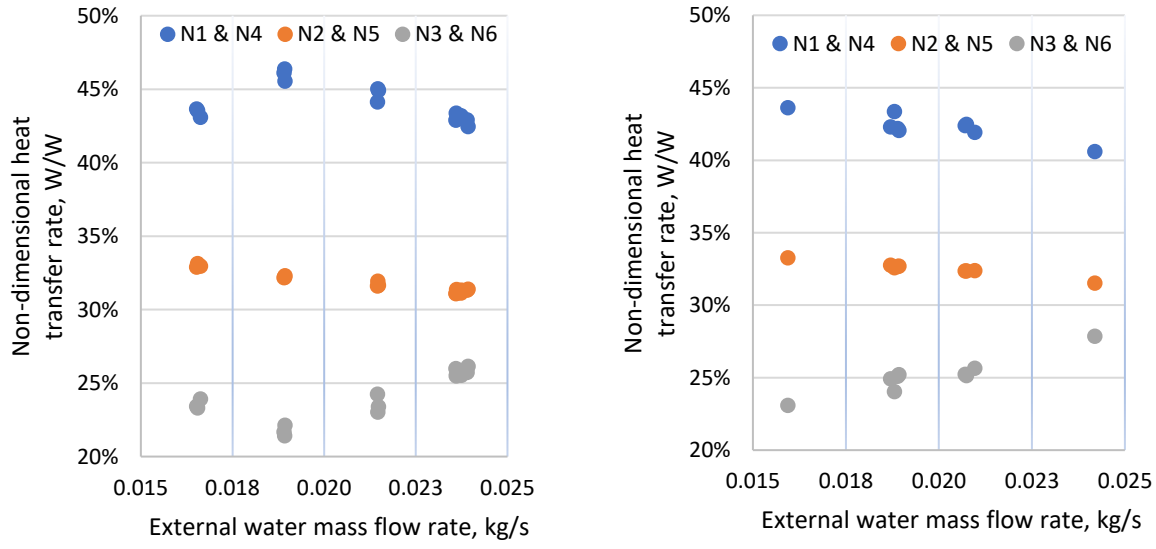

a) Inlet water temperature T_i = 45 °C b) Inlet water temperature T_i = 50 °C

Figure 6 a) Non-dimensional heat rate of each group of heat exchanger plates as a function of external mass flow rate.

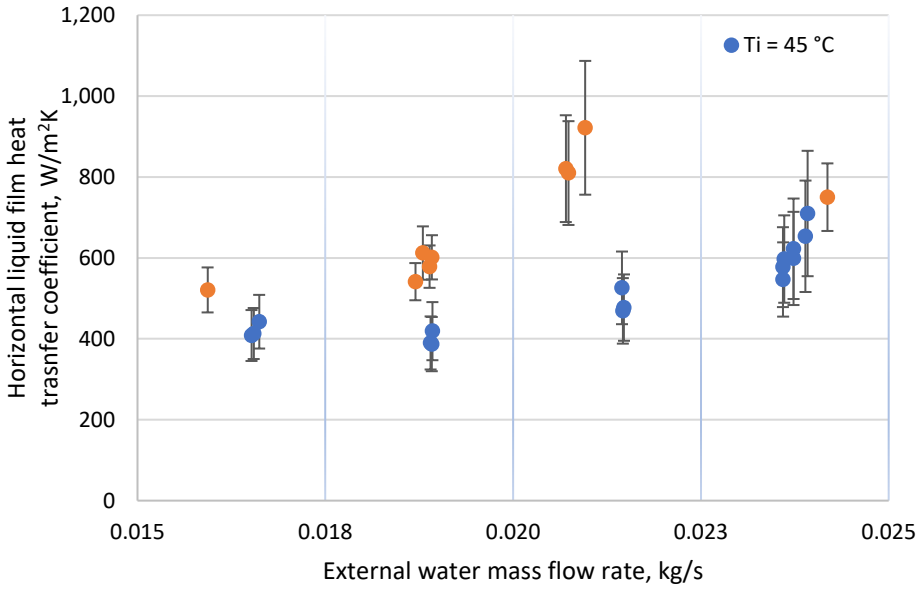

Figure 7 Horizontal liquid film heat transfer coefficient as a function of the external mass flow rate.

Finally, Fig. (7) shows the horizontal liquid film heat transfer coefficient as a function of the external mass flow rate. A maximum heat transfer coefficient of α_f = (921 ± 165) W/m^2°C was achieved on the horizontal liquid film, which is slightly lower compared to the conventional falling film tube bundle from the literature review (3000-5000 W/m^2°C). Falling film heat transfer coefficients are high due to the low liquid film thickness, which is approximately 200 µm. The thermal resistance of the liquid film is lower compared to the present work, which has a higher horizontal liquid film thickness. However, when analyzing the global heat transfer coefficient, the performance seems to be similar. It may be explained that although the new heat exchanger proposal was characterized by a lower local heat transfer coefficient range, the total area wettability may compensate for the overall heat transfer coefficient. In summary, the thermal resistance of the horizontal liquid film thickness accounts for about 90 % of the total thermal resistance due to the high convective heat transfer coefficient for the water coolant (α_c = 15616 ± 785 W/m^2°C) compared to α_f. Additionally, the heat transfer coefficient increased as external mass flow rate increased.

5. CONCLUSIONS

A new horizontal liquid film heat exchanger was experimentally studied. An α_f = (921 ± 165) W/m^2°C maximum heat transfer coefficient on the horizontal liquid film was achieved, which is slightly low in comparison the conventional falling film tube bundle from the open literature review. However, the performance seems similar when the global heat transfer coefficient was analyzed. It may be explained that although the new heat exchanger proposal was characterized by a lower heat transfer coefficient range, the total area wettability may compensate for the overall heat transfer coefficient. Summarizing, the thermal resistance of the horizontal liquid film thickness is about 90 % of the total thermal resistance, due to the convective heat transfer coefficient for the water coolant is high α_c = (15000 ± 785) W/m^2°C as compared from α_f. Furthermore, the heat rate of the first group of heat exchangers (N1 and N4) represents about 40 % of the total heat of absorption. Finally, a simultaneous heat transfer analysis along with a hydrodynamic investigation should carried out in the new proposal because the horizontal liquid film thickness strongly affect the heat transfer performance as showed by Narváez-Romo and Simões-Moreira [2].

6. ACKNOWLEDGEMENTS

Authors would like to thank to the Sao Paulo Research Foundation (FAPESP) for the project funding - Grant No. 2016/09509-1. Moreover, the first author thanks Program SGA-USPSustent for the personal financial support.

NOMENCLATURE

A	area, [m^2]
c_p	specific heat capacity, [J/kgK]
D	diameter, [m]
f	friction factor, [-]
k	thermal conductivity, [W/mK]
L	length, [m]
$\dot{m}$	length, [kg/s]
N	plate number, [-]
Nu	Nusselt number, [-]
Pr	Prandtl number, [-]
$\dot{Q}$	heat rate, [W]
Re	Reynolds number, [-]
T	temperature, [°C]

Greeks

α	heat transfer coefficient, [W/m^2K]
μ	dynamic viscosity, [Pa s]

Subscripts

avg	average
i	inlet
o	outlet
c	coolant circuit
f	horizontal film

7. REFERENCES

Chyu, M. C., Bergles, A. E., An analytical and experimental study of falling-film evaporation on a horizontal tube. *Journal of Heat Transfer*, vol. 109, no. 4, pp. 983–990, (1987).

Dittus, F. W. Heat transfer in automobile radiators of the tubler type. Univ. Calif. Pubs. Eng., v. 2, p. 443, (1930).

Fernandes, J. R., Baptista, M. S., Cunha, J. P., Maia, J. M., Wettability effects on falling film evaporation in a horizontal tube. *Applied Thermal Engineering*, 115, 529-537, (2017).

Gnielinski, V. New equations for heat and mass transfer in turbulent pipe and channel flow. *Int. Chem. Eng*., v. 16, n. 2, p. 359–368, (1976).

Hu, X., and Jacobi, A. M., The Intertube Falling Film: Part 2 - Mode Effects on Sensible Heat Transfer to a Falling Liquid Film, *Journal of Heat Transfer*, vol. 118, no. 3, pp. 626–633, (1996).

Klein, S. Engineering Equation Solver (EES) V9, F-chart software, Madison, USA. (2015).

Lienhard, J. H. IV., & Lienhard, J. H. V., *A Heat Transfer Textbook* (4th ed.). Phlogiston Press, (2011).

Narvaez Romo B. *An experimental study of an ammonia-water absorption refrigeration cycle using a novel modified horizontal liquid film absorption system.* Ph.D. Thesis, University of Sao Paulo, (2020).

Narváez-Romo, B., Simões-Moreira, J. R., Falling liquid film evaporation in subcooled and saturated water over horizontal heated tubes. *Heat Transfer Engineering*, 38(3), 361-376, (2017).

Narváez-Romo, B., Zavaleta-Aguilar, E. W., Simões-Moreira, J. R. Heat and mass transfer in falling films technology applied to the generator and the rectifier of an ammonia-water absorption refrigeration cycle. International Journal of Refrigeration, 135, 276-287, (2022).

Ong, K. C. G., Bao, R., Thorpe, R., Critical heat flux enhancement in falling film evaporation of pure water on structured surfaces. International Journal of Heat and Mass Transfer, 143, 118576, (2019).

Ribatski, G., Jacobi, A. M. Falling-film evaporation on horizontal tubes - A critical review. *Int. J. Refrigeration*, 28(5), 635–653, (2005).

Varón, L.M.V., Narváez-Romo, B., Costa-Sobral, L., Barreto, G., Simões-Moreira, J.R. Novel high-flux indoor solar simulator for high temperature thermal processes, *Applied Thermal Engineering*, 2023, 121188,

Xu, J., Wang, Z., Zhang, X., He, Y. (2020). Wettability enhancement and its effect on flow patterns and heat transfer in falling film evaporation. *Applied Thermal Engineering*, 164, 114509.

Zhang, M., Wu, D., Hu, Y., Wang, W. Effects of microstructure-textured surface on heat transfer characteristics of falling film evaporation. *International Journal of Heat and Mass Transfer*, 171, 121182, (2021).

8. RESPONSIBILITY NOTICE

The author(s) is (are) the only responsible for the printed material included in this paper.